# Physical Transport in the Culebra Dolomite

by Lucy C. Meigs and James T. McCord

7/11/96





5

# Physical Transport in the Culebra Dolomite

The Culebra Dolomite Member of the Rustler Formation is being studied as a possible transport medium for radionuclides released from the WIPP repository by future inadvertent human intrusion. This letter report describes data collection and data analyses which led to our current conceptual model of physical transport in the Culebra. It also covers how the conceptual model is implemented in the performance assessment (PA) of the WIPP site, and parameterization of the PA numerical models of physical transport in the Culebra.

## Characterization of the Culebra for Development and Testing of Conceptual Models

In order to determine the important processes (advection, dispersion and diffusion) controlling contaminant transport and to evaluate the physical transport properties of the Culebra dolomite, a series of tracer tests has been conducted. Among the most important issues is whether the Culebra should be modeled as a single-porosity medium with transport only in the fractures or whether there may be significant interaction with the "matrix" (double-porosity medium). Convergent-flow tracer tests were conducted within the Culebra at three locations (H-3, H-6, and H-11 hydropads) between 1981 and 1988. These tests showed rates and amounts of solute transport to be strongly dependent on flow direction, and suggested that a physical retardation mechanism was affecting transport. The tracer-breakthrough curves from these tests were simulated using a homogeneous double-porosity continuum model (SWIFT II). These simulations showed that the observed transport behavior could be explained by a combination of anisotropy in horizontal hydraulic conductivity and matrix diffusion. These tests ruled out conceptualizing the Culebra as a homogeneous single-porosity medium (Jones et al., 1992). However, significant questions remained as to whether other processes such as heterogeneity in hydraulic conductivity could have caused the tailing in the breakthrough curves that was attributed to matrix diffusion.

Additional tracer tests have recently been conducted at the H-11 and H-19 hydropads. These tests included single-well injection-withdrawal tests and multiwell convergent-flow tests at both locations. The results of a preliminary tracer test conducted May-July 1995 at the H-19 hydropad revealed that at this site, transport was slower than at previous sites tested. The relatively high advective porosity (greater than 0.05, larger than typical fracture porosities) that appears to be required to model these data caused us to question our previous conceptualization of the Culebra. Through careful reexamination of the geology and stratigraphy of the Culebra, we have developed a clearer picture of the important processes that control transport.

The Culebra has non-uniform properties both horizontally and vertically. This has been demonstrated with both hydraulic and tracer tests. The upper portion of the Culebra has a much lower permeability and does not appear to provide pathways for rapid transport (see effective thickness discussion below). Examination of core and shaft exposures has





6

revealed that there are multiple scales of porosity within the Culebra including: fractures ranging from microscale to potentially large, vuggy zones, and interparticle and intercrystalline porosity (Figure 1). Flow occurs within fractures, within vugs where they are connected by fractures, and probably to some extent within interparticle porosity where the porosity is high, such as "chalky" lenses. At any given location, flow will occur in response to hydraulic gradients in all places that are permeable. The variation in peak arrival time in tracer breakthrough curves between the H-11 and the H-19 hydropads suggests that the types of porosity contributing to rapid advective transport vary spatially. In addition to advective transport of solutes, diffusive transport will occur into all connected porosity. Thus, diffusion can be an important process for effectively retarding solutes by transferring mass from the porosity where advection (flow) is the dominant process into other portions of the rock. Diffusion into stagnant portions of the rock also provides access to additional surface area for sorption. When the permeability contrast between different scales of connected porosity is large, transport can effectively be modeled by dividing the system into advective porosity (often referred to as fracture porosity) and diffusive porosity (often referred to as matrix porosity).

The interpretations of tracer test data to date have relied on both homogeneous and heterogeneous single- and double-porosity continuum models (SWIFT II and THEMM). Spatial variations in advective transport are represented in numerical simulations of the tracer tests with random fields of hydraulic conductivity. Interpretations completed thus far have shown that the single-well injection-withdrawal test data from both the H-11 and H-19 hydropads cannot be explained by heterogeneity alone. Simulations of cumulative mass recovery during the withdrawal phase of the single-well tests with both homogeneous and heterogeneous models suggest that mass recovery should be very rapid for single-porosity media. The Culebra tracer test data, however, show a much slower cumulative mass recovery, as would be anticipated if some sort of diffusional process was controlling mass recovery (i.e. if matrix diffusion is playing a significant role).

In summary, the major physical transport processes that affect actinide transport through the Culebra dolomite include advection (through fractures and other permeable porosity), dispersive spreading during advection due to heterogeneity, and matrix diffusion (between fractures and matrix or more generally, diffusion between adjacent regions with large permeability contrasts). Sorption also exerts an important control on transport, however this memorandum focuses on physical transport rather than chemical transport.

PA Modeling of Physical Transport in the Culebra

At the Performance Assessment (PA) scale, spatial variability in advective transport is represented by heterogeneous transmissivity fields that have been conditioned on available point transmissivity data and transient pressure data. In the PA calculations, the lower permeability of the upper portion of the Culebra has been approximated by eliminating this portion of the Culebra from the transport model. The possible spatial variability in transport properties (diffusion and sorption rates) has not been taken into





7

Figure 1. Multiple scales of Culebra porosity based on examination of core, shaft mapping and RaaX logging (Holt, 1996).

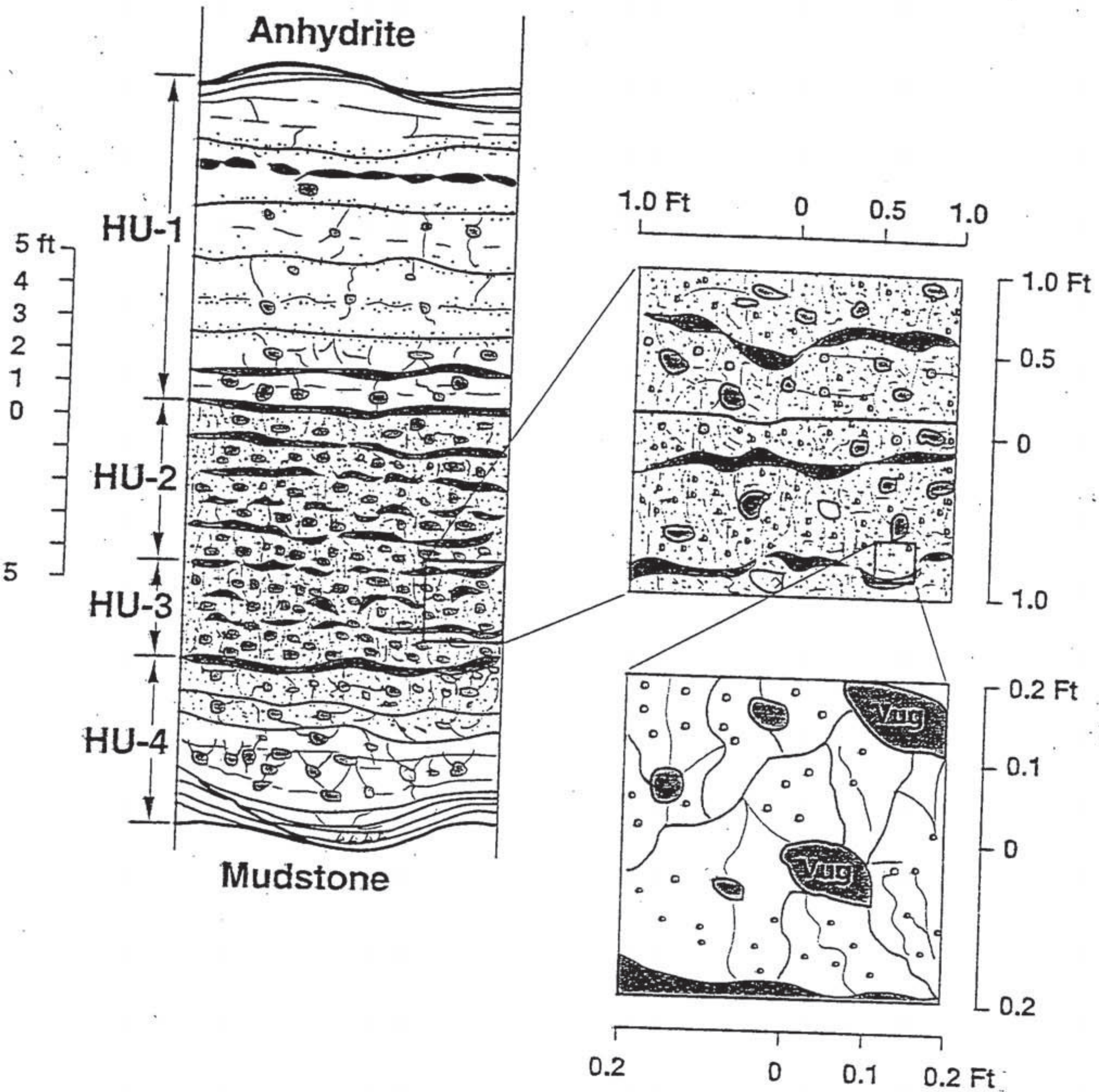






8

account in the PA model. Attempts have been made to take into account the variability by limiting the parameter ranges to the expected effective spatial averages across the site and, when unquantified uncertainties exist, by providing conservative estimates of transport parameters (i.e. parameters that could lead to greater releases than expected). For instance, with respect to effective Culebra thickness (see next section), field data indicate that only the lower 4± m actively participates in flow at most locations sampled. Despite the fact that our rather sparse sampling network prevents us from ruling out the existence of regions where the entire 7 m of Culebra is active in the physical transport process, we have conservatively specified that PA calculations should consider the Culebra to be only 4 m thick everywhere.

The PA for WIPP models transport in the Culebra with SECOTP2D which is a double-porosity model. The physical transport parameters required by SECOTP2D are: (1) effective thickness (See parameter records package in the Sandia WIPP Central Files (SWCF-A), WPO#37223), (2) advective porosity (often referred to as fracture porosity) (WPO#37227), (3) diffusional porosity (often referred to as matrix porosity) (WPO#37228), (4) half matrix block length (defined as one-half the thickness of a matrix slab between two parallel plate fractures) which represents specific surface area to volume ratio for matrix diffusion (WPO#37225), (5) diffusive (or matrix) tortuosity (WPO#37226), and (6) dispersivity (WPO#s 37230 and 37231). Effective thickness, diffusive porosity, and diffusive tortuosity were all specified based on field or laboratory measurements. Half matrix block length and advective porosity were specified based on the interpretation of tracer test data from the H-3, H-11 and H-19 hydropads (Hydro Geo Chem, Inc., 1985; Stensrud et al., 1990, Beauheim et al., 1995). Dispersivity values were developed based on comparison of values inferred from tracers tests to large-scale values expected due to heterogeneity at the PA scale. A description of the rationale for the distribution of each of these parameters is provided below.

*Effective Thickness*

The effective thickness used for the SECOTP2D calculations is 4.0 m. This effective thickness represents the median Culebra total thickness within the land withdrawal boundary (LWB) (7 m) minus the median (and mean) thickness of Unit 1 (upper Culebra) within the LWB (3 m) as defined by Holt (1996). There is considerable information that indicates that there are significant vertical stratigraphic variations in the Culebra (Holt and Powers, 1984, 1986, 1988, 1990). Based on the descriptions of numerous cores it can be concluded that the basic stratigraphy of the Culebra dolomite is continuous across the land withdrawal boundary area (Holt, 1996; Holt and Powers 1988). Recent hydraulic tests at the H-19 hydropad (Kloska et al., 1995) have indicated that the permeability of the upper portion of the Culebra is significantly lower than the permeability of the lower Culebra at this hydropad. Hydrophysical (fluid) logging also suggest that most of the flow is coming from the lower portion of the Culebra at H-19 (Results of COLOG work, WPO# 38402). Tracer tests have confirmed that at the H-19 hydropad the upper portion of the Culebra does not play a significant role in solute transport. Tracers injected into





9

the upper Culebra at H-19b3, H-19b5, H-19b7 only showed up at the pumping well (H-19b0) at barely detectable levels, whereas tracers injected into the lower Culebra or the full Culebra at these wells showed up at the pumping well in significant concentrations (Beauheim et al., 1995; and H-19 tracer test data (WPO# 37452)). In descriptions of the Culebra dolomite in the Air Intake Shaft, Holt and Powers (1990) noted that most of the fluid observed to come out of the Culebra came from the lower portion of the Culebra. Mercer and Orr (1979) report the results of a tracer ($^{131}I$) and temperature survey run at the H-3 hydropad which indicated that, within the resolution of the test, 100 percent of the flow out was in the lower approximately 10 ft of the Culebra. This test thus suggests that at H-3 the upper 14 ft of Culebra has a very low permeability. Hydraulic testing at well H-14 found that at this location the permeability of both the upper and the lower Culebra was quite low. At H-14 the permeability of the upper Culebra is slightly higher than the permeability of the lower Culebra (Beauheim, 1987). In summary, the bulk of the data points to the fact that in many locations the majority of the flow and transport appears to be taking place in the lower portion of the Culebra, i.e. excluding hydrostratigraphic unit 1. There may be locations where the entire Culebra participates in transport, but for lack of evidence along the off-site pathway, a thinner thickness has been selected. If additional evidence were to be collected that indicated that the entire Culebra thickness should be used in the PA model, the use of this larger thickness would result in slower transport and a decrease in releases.

*Diffusive Porosity*

The diffusive porosity distribution used for the SECOTP2D calculations is:

| | |
|---|---|
| Minimum | 0.10 |
| 10th Percentile | 0.11 |
| 25th percentile | 0.12 |
| 50th percentile | 0.16 |
| 75th percentile | 0.18 |
| 90th percentile | 0.19 |
| Maximum | 0.25 |

This porosity distribution is derived from laboratory measurements. Boyle's Law helium porosity measurements have been made on 103 Culebra core plugs from 17 locations as reported in Kelley and Saulnier (1990), as well as additional porosity measurements recently completed by Terra Tek (WP0#38234). Water resaturation porosity measurements were also made for a subset of the cores. All measurements were very similar; the average difference between the water resaturation porosity and the Boyle's Law helium porosity was less than 0.005. The methodology used for these porosity measurements and the comparisons made are described in Kelley and Saulnier (1990). A spreadsheet in the diffusive porosity parameter records package (WPO#37228) summarizes all the Boyle's Law helium porosity data that have been collected. This spreadsheet summarizes the maximum, minimum, median and average for all data, data averaged by well, and well averages averaged by hydropad, and all data averaged by hydropad. The hydropad averages of the data were used to develop the distribution presented above since the wells at an individual hydropad are very close together as compared to the spacing of all wells. As expected, averages from the hydropads give a narrower distribution than the distribution of all data. In the PA simulations (SECOTP2D), a single value of diffusive porosity is used across the entire model domain for a given realization. The value used for diffusive porosity clearly should be the effective average diffusive porosity encountered along the expected off-site pathway. Thus it does not make sense to include the extreme individual data values in the distribution for use by PA.

*Diffusive Tortuosity*
The diffusive tortuosity used for the SECOTP2D calculations is 0.11. This tortuosity value is the median tortuosity calculated from 36 core measurements at 13 locations as reported in Kelley and Saulnier (1990) together with additional measurements recently completed by Terra Tek (WP0#38234). (The measurements reported by Kelley and Saulnier (1990) were also made by Terra Tek.) Terra Tek first determined the formation factor based on electrical-resistivity measurements of core plugs. The formation factor results subsequently were used to calculate tortuosity. Tortuosity is a measurement of the tortuous nature of the pore structure within the rock. The smaller the value, the more tortuous the pathway and the slower the diffusion rate. The methodology used for the determination of formation factor and the calculation of tortuosities is described in Kelley and Saulnier (1990). A spreadsheet in the diffusive tortuosity parameter records package (WPO#37226) summarizes all the tortuosity data. Diffusive tortuosity is fixed parameter in PA calculations because there is a relatively small range to the data with few outliers.

*Half Matrix Block Length*
The matrix half-block length distribution used for the SECOTP2D calculation is a uniform distribution ranging from 0.05 to 0.5 m (i.e., full matrix block length values from 0.1 to 1.0 m), with a single value drawn from this distribution for each realization (implying that a single sampled value should represent an average of spatially variable block lengths along the expected "off-site pathway"). This distribution is derived from results of simulating the tracer tests conducted at the H-3, H-11, and H-19 hydropads. Numerical simulations were performed with double-porosity continuum models with both homogeneous and heterogeneous hydraulic conductivity fields. The homogeneous approach utilized the SWIFT-II transport code, and the heterogeneous approach used the THEMM code; both are being qualified per WIPP QAP 19-1. (See WPO#37450 for additional information on simulations.)

Both modeling approaches yielded consistent results for each well-to-well path with regard to matrix block length. It should be pointed out that for some paths the best fit block length is somewhat smaller than the minimum value of the range (e.g., H-11b2), and for some paths the best fit is larger than the recommended range (e.g., H-3b1) for the PA distribution. However, as mentioned above, the PA distribution is really a distribution of expected spatial averages, since each realization utilizes a single value for block length for the entire simulation domain. It is also important to remember that the tracer test results reflect transport behavior over paths of lengths represented by the well spacing, or lengths ranging from 10 to 30 meters. Considering these two facts, the entire range of matrix block length values inferred from the tracer tests has been truncated to yield the PA distribution which ranges uniformly from 0.1 to 1.0 m. Any single value drawn from the distribution should represent an aerial average for the exit pathway of 2.5 km length, roughly the distance from the center of the waste panels to the land withdrawal boundary. We strongly feel that the extreme value of matrix block greater than 1.0 m will not occur over regions as large as the exit pathway. It should be noted that simulations with a large matrix block length (small surface area for diffusion) will lead to more releases (compared to simulations with small matrix block lengths) because there will be less diffusion and in turn less accessible surface area for sorption.

In general, the matrix block length and advective porosity were the two primary fitting parameters inferred from comparing simulation results to field data. This is because essentially all of the other physical transport parameters could be measured independently with semi-quantifiable and rather small uncertainties; these other parameters were thus considered "fixed values" in the simulations (See WPO#37439). In an effort to obtain extreme values for matrix block length (as well as advective porosity), some of the interpretive simulations stressed the fixed parameters towards the endpoints of their uncertainty range. The "stressing" of fixed parameters was performed in a deliberate fashion such that all changes to the fixed values would "push" the fitted parameter value in the same direction. For instance, to obtain the minimum matrix block length one would decrease the well spacing, the free-water diffusion coefficient and the diffusive porosity, and increase the pumping rate. Simulations with stressed parameters were only conducted for those pathways that had either very large or very small block lengths for the best fit simulations with the fixed parameters at our best estimate. The best-fit matrix block lengths for the stressed simulations lie at or beyond the endpoints of the best-fit distribution (and well beyond the endpoints of the recommended PA distribution). Again, as alluded to in the preceding paragraph, while such extreme values of matrix block length may be valid for simulating transport in the Culebra at some locations within the WIPP simulation domain, it is considered highly unlikely that they occur over regions approaching the length scale of the entire exit pathway. Thus the recommended PA distribution for aerially-averaged matrix block length has endpoints less extreme than the hydropad-scale fitted values. A uniform distribution is recommended because it gives equal probability to all values within the distribution. Even though tracer test interpretations to date suggest that there may be a somewhat higher probability that the block length should be at the lower end of the distribution, given the facts that we have only a limited number of tests sites and that smaller block lengths will yield slower travel paths to the PA compliance boundary (e.g., more physical retardation), we have chosen to recommend a uniform distribution.





12

One final note which must be addressed relates to the fact that the PA model (SECOTP2D) utilizes a parallel plate model for simulating double-porosity (fracture and matrix) transport, whereas our tracer test interpretive tools (SWIFT II and THEMM) utilize spherical models for simulating the matrix block geometry. (The matrix block length is conceptualized as the thickness of a matrix block between two fractures and represents the surface area to volume ratio for diffusion between the advective porosity and the diffusive porosity.) One important consideration results from this difference in conceptualization of physical retardation via matrix diffusion. This consideration is important with respect to matrix diffusion parameters, particularly when the time scale of a solute pulse duration is small with respect to the diffusion time scale for solute to move from the fracture-block interface to the center of the block. When the pulse duration time scale is small compared to the diffusion-to-block-centroid time scale (e.g., relatively large blocks), the diffusing solute never "feels" solute diffusing in from the other side of the block and it behaves as if it is diffusing into an infinite length block. In these cases, the surface area for diffusion determines the diffusion rate and one can directly convert from the spherical model to the parallel plate model by dividing the block length determined using the spherical blocks by three. On the other hand, when the diffusion-to-block-centroid time scale is equal to or less than the pulse duration time scale (e.g., for relatively small blocks, or long solute pulse durations), solutes invading matrix blocks from opposite sides "meet" at the centroid, resulting in decreased concentration gradients and concurrent decreases in physical retardation due to decreased matrix diffusion. When the blocks become saturated, the spherical and parallel plate block model block lengths can be considered equivalent. At this limit, the double-porosity transport model converges on a single porosity model with all of the pore space (advective + diffusive porosity) immediately accessible by solutes (thus no fast fracture flow paths with rapid transport to the compliance boundary). Between the extremes of large blocks with essentially infinite diffusion and small blocks which allow immediate complete solute saturation of all porosity (equivalent to single-porosity with high porosity), the block length obtained by a spherical model would be between 1-3 times larger than that that would be obtained with a parallel plate model. Given that the conversion between spherical and parallel plate models depends on the parameters of the simulation, that we expect the smaller block sizes in the distribution given to PA to have small diffusion time scales compared to expected pulse duration's time scales, and that the larger blocks will yield faster travel paths to the PA compliance boundary with less physical retardation, we have chosen not to divide our block lengths by three for the recommended PA distribution.

*Advective Porosity*

The advective porosity distribution used for the SECOTP2D calculation is log-uniform over a range from $1x10^{-4}$ to $1x10^{-2}$. This distribution was derived from numerical simulation of the tracer tests conducted at the H-3, H-11, and H-19 hydropads, and comparing simulated to observed tracer breakthrough data at the pumping well. As mentioned above for matrix block length, two different double-porosity conceptual





13

models were applied, a homogeneous media approach and a heterogeneous media approach. The homogeneous approach utilized the SWIFT-II transport code, and the heterogeneous approach used the THEMM code. (See WPO#37450 for additional information on simulations.)

Both modeling approaches yielded consistent results for each well-to-well path with regard to advective porosity. As was the case for matrix block length, for some paths the best-fit advective porosity is somewhat smaller than the minimum value of the range (e.g., H-11b3) and for some paths the best fit is larger than the recommended range (e.g., H-19b2, b3, b4, b5, b6, b7). It is important to remember that the tracer test results reflect transport behavior over paths of lengths represented by the well spacing, or lengths ranging from 10 to 30 meter. The entire range of best fit values from the tracer tests has been truncated for the PA distribution based on the fact that the PA transport model utilizes a single value for advective porosity for the entire simulation domain. Recall that single value should represent an aerial average for the exit pathway. We strongly feel that the extreme values of advective porosity less than $1x10^{-4}$ will not occur over regions as large as the exit pathway, and thus aerial averages lie between these two endpoints. It should be noted that simulations with a small advective porosity will lead to more releases (compared to simulations with large advective porosity) because there will be faster transport resulting in less time for diffusion and in turn less accessible surface area for sorption.

As mentioned above, the advective porosity and matrix block length were the two primary fitting parameters inferred from comparing simulation results to field data. Again, in an effort to obtain extreme values for matrix block length and advective porosity, some of the interpretive simulations stressed the fixed parameters towards the endpoints of their uncertainty range. The "stressing" of fixed parameters was performed in a deliberate fashion such that all changes to the fixed values would "push" the fitted parameter value in the same direction. Simulations with stressed parameters were only conducted for those pathways that had either very large or very small block lengths for the best fit simulations with the fixed parameters at our best estimate. The best-fit advective porosity for the stressed simulations lie at or beyond the endpoints of the best-fit distribution (and well beyond the endpoints of the recommended PA distribution). Again, as alluded to previously, while such extreme values of advective porosity may be valid for simulating transport in the Culebra at some locations within the WIPP simulation domain, it is considered highly unlikely that they occur over regions approaching the length scale of the entire exit pathway. Thus the recommended PA distribution for aerially-averaged advective porosity has endpoints less extreme than the hydropad-scale fitted values. A log uniform distribution is recommended because it gives equal probability to all values in log space. There is not sufficient data from the three hydropad test sites to create a meaningful probability distribution other than log uniform. Two of the tracer test sites have a relatively low advective porosity and one site has a high advective porosity.

*Dispersivity*

For the PA transport simulations using SECOTP2D, we recommend using a longitudinal and transverse dispersivity equal to zero. If, for numerical stability and/or convergence reasons, a non-zero value is desired, we recommend a constant value of 2 m or smaller. For simulations using a non-zero longitudinal dispersivity, we recommend a longitudinal to transverse dispersivity ratio of 10:1. The rationale for this recommendation lies in the fact that dispersive spreading due to permeability heterogeneity at the PA scale appears to overwhelm dispersive mixing observed at smaller (e.g., hydropad) scales (see detailed discussion below). Given that PA models for flow and transport in the Culebra explicitly account for heterogeneity in the permeability fields, there is no need to specify a discrete dispersivity value to account for mixing at the PA and smaller scales.

Research into solute dispersion in groundwater over the past couple of decades has identified a characteristic trend in dispersivities over a wide range of length scales of interest. The trend clearly shows that dispersivity tends to increase as one moves from a labortory column scale (cm) to the field scale (m), with larger field problems exhibiting generally higher dispersivity than smaller field problems. This trend perhaps is best summarized by the well-known Gelhar figure (e.g., Gelhar, 1986; Gelhar et al., 1992) in which lab and field data from a large number of experiments are presented on a single plot; this plot is reproduced here as Figure 2. This figure clearly shows the longitudinal dispersivity, $\alpha_l$, increasing with the scale of the problem. Also shown in the plot are dashed curves which approximate the min-max envelope of the data and the straight line $\alpha_l=0.1L$ where $L$ is the length scale of the experiment domain. The $\alpha_l=0.1L$ line represents the "rule of thumb" often employed when one simulates field-scale problems without the luxury of having site-specific field-scale dispersivities. Notable for the purpose of the WIPP PA simulations is the fact that at scales greater than 1 km, all data values fall below the *0.1L* line (most of them substantially below the line with values ranging from *0.01L* to *0.001L)*.

For the WIPP PA, we are interested in transport from the waste panel area to the land withdrawal boundary (LWB). For the most likely curvilinear exit trajectories, this distance is on the order of 2.5 to 3 km. Unfortunately, our largest scale site-specific data for the dispersivity of the Culebra is from the hydropad tracer tests, with well spacings ranging between 10 and 43 m. When intepreting the results of hydropad tracer tests conducted in the Culebra, best fits with homogeneous media models generally used dispersivities less than or equal to *0.1L*. Furthermore, hydraulic testing at the hydropad sites yielded estimates of the lnK variance ($\sigma_{\ln K}^2$) and lnK correlation scale ($\lambda$) product of less than 1.5 m. Stochastic analyses of flow and transport in heterogeneous aquifers (e.g., Gelhar, 1986) derive this product as an estimator of asymptotic macrodispersivity, $\sigma_{\ln K}^2 \cdot \lambda = \alpha_l$. In summary, hydraulic and tracer testing of the Culebra dolomite at the WIPP site indicate that at the hydropad scale the dispersivity is generally less than 2 m. Based on Figure 2, at a length scale of an exit trajectory from the waste panels to the LWB (~3

Figure 2. Laboratory and field measured values of longitudinal dispersivity as a function of scale of measurement. The largest circles represent the most reliable data (Adapted by Fetter, 1993, from Gelhar, 1986).

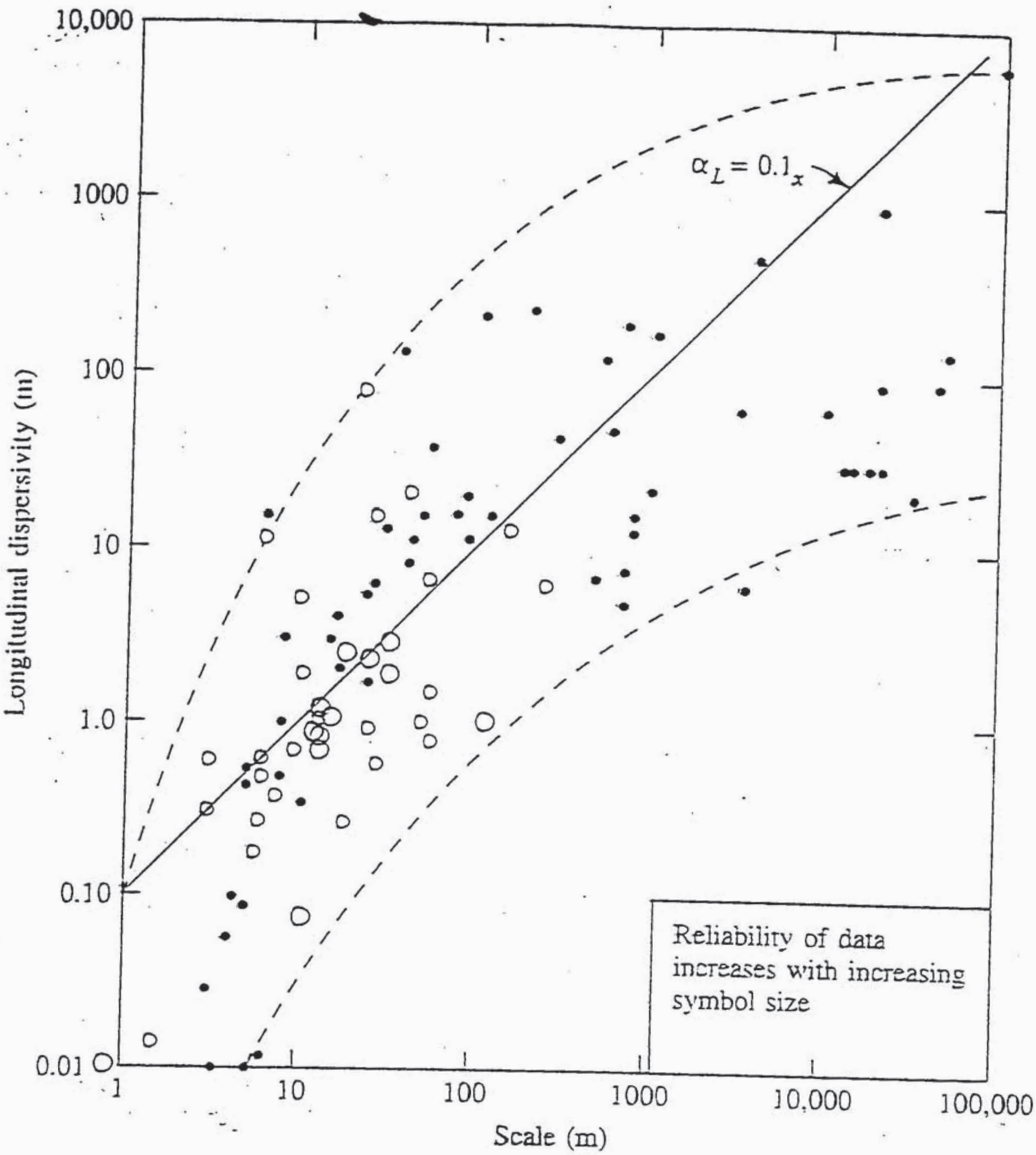






16

km) we would expect dispersivities to range somewhere between 10 and 1000 m (or a normalized dispersivity $A=\alpha/L$ to vary between .0033 and 0.33).

This gross estimate of large scale dispersivity derived from Figure 2 can be compared to site-specific spreading estimates using the PA flow model. The PA groundwater flow and transport simulations explicitly acknowledge heterogeneity in the Culebra permeability fields by providing a gridblock by gridblock variation in permeability , with that variation conditioned on permeability measurements/observations from hydropad scale hydraulic testing (i.e., T-fields generated by GRASP-INV, see Appendix TFIELD). One can estimate the effective dispersivity associated with the heterogeneous permeability fields by tracking particles from the source (waste panel) area to the exit (LWB) location, and computing the temporal statistics of the particle travel time from source to exit. Equation 10.7 in Domenico and Schwartz (1990) show that one can use the temporal statistics to compute the dispersivity from such a particle tracking exercise:

$$\alpha_l = \frac{v\sigma_t^2}{2t} \qquad (1)$$

where $v$ is the average pore water velocity (computed as the distance divided by the mean travel time), $\sigma_t^2$ is the variance of particle travel time, and $t$ is the mean travel time. We implemented this approach by tracking particles released along a line in the middle of the waste panel area (with the line parallel to the LWB) to the Land Withdrawal Boundary, and the particle tracking results yielded the input parameters required for equation 1 ($\sigma_t^2$ and $t$). This particle tracking was performed on all 100 heterogeneous permeability field realizations generated by GRASP-INV for the 1996 PA (undisturbed by mining). Results of this particle tracking approach show heterogeneity-induced spreading to yield PA-scale dispersivities ranging from approximately 10 m to approximately 1000 m (normalized values between .003 and 0.3). This result is entirely consistent with published results from other experiments conducted around the world published before 1992 (e.g., Figure 2), and these dispersivities are significantly larger than those inferred from the hydropad tracer test results. We therefore feel that, given no site-specific large-scale data on dispersivities, we can trust that the transmissivity heterogeneity explicitly accounted for in the Culebra flow (SECOFL2D) simulations will impart a reasonable amount of dispersive solute spreading on simulated actinide releases with no need to specify additional spreading through the dispersivity parameter in SECOTP2D.

Gelhar et al. (1992) also summarize experimental results related to transverse dispersivity, and they show that the ratio of longitudinal to (horizontal) transverse dispersivity generally ranges between 2:1 and 50:1 and exhibits no clear trend with problem scale. For the WIPP site, no definitive / highly reliable data set exists to provide an estimate of transverse dispersivity. Again, we feel that the heterogeneity in the flow simulations will cause a reasonable amount of spreading, and we should not take credit for additional spreading by specifying a dispersivity for SECOTP2D which exceeds that caused by the transmissivity heterogeneity.

Based on the above data, analysis, and discussion, any specified value of longitudinal dispersivity less than roughly 2 m will yield similar results for solute transport in the Culebra dolomite from the WIPP waste panel area to the LWB. Assuming that the numerical codes used correctly solve the governing partial differential equations, simulations using local dispersivities less than or equal to 2 m will yield results consistent with field-scale dispersive spreading observations as reported by Gelhar et al. (1992). Given the lack of WIPP site-specific information related to transverse dispersivity, we rely entirely on previous studies (e.g., see Gelhar et al., 1992) to recommend a ratio of longitudinal to transverse dispersivity equal to 10:1.

*Parameter Cross Correlations*

One might suspect the possibility of some cross correlation between sampled parameters. To test this suspicion, we have prepared scatter plots of interpreted results from the hydropad test sites which yielded the physical transport parameters used to develop the PA parameter distributions (H-3, H-11, and H-19). Scatter plots of well-to-well transmissivity versus well-to-well advective porosity and matrix block length showed no observable trends, nor did a scatter plot of advective porosity versus matrix block length . These results strongly suggest a lack of correlation between these parameters, and therefore the recommended PA distributions include no cross correlations.

*References*


Beauheim, R. L. 1987. *Interpretations of Single-Well Hydraulic Tests Conducted at and Near the Waste Isolation Pilot Plant (WIPP) Site, 1983-1987.* SAND87-0039.

Beauheim, R. L., L.C. Meigs, G.J.Saulnier, and W.A. Stensrud, 1995. Culebra Transport Program Test Plan: Tracer Testing of the Culebra Dolomite Member of the Rustler Formation at the H-19 and H-11 Hydropads on the WIPP Site.(Tracer test data will be in WPO#s 37452, 37467, and 37468.)

Cauffman, T.L., A.M. and J.P. McCord. 1990, *Ground-Water Flow Modeling of the Culebra Dolomite*, Volume II: Data Base. SAND89-7068/2

Domenico, P., and F.W. Schwartz, 1990. *Physical and Chemical Hydrogeology*, John Wiley Publishing.

Fetter, C.W., 1993. *Contaminant Hydrogeology*, Macmillan Publishing Co., 458 pp.

Gelhar, L.W., 1986. Stochastic subsurface hydrology from theory to applications, *Water Resources Research* , v.22(9): 135s-145s.

Gelhar, L.W., C. Welty, and K. Rehfeldt, 1992. A critical review of data on field-scale dispersion in aquifers, *Water Resources Research*, v.28(7): 1955-1974.

Hydro Geo Chem, 1985. *WIPP Hydrology Program, Waste Isolation Pilot Plant, SENM, Hydrologic Data Report #1*, SAND85-7206, 710pp.

Holt, R.M. 1996. unpublished letter report entitled *Hydrostratigraphy of the Culebra Dolomite Member of the Rustler Formation in the WIPP Region* (WPO#38225).

Holt, R. M. and D.W. Powers, 1984, *Geotechnical Activities in the Waste Handling Shaft*. WTSD-TME-038, U.S. Department of Energy by TSC and International Technology Corporation

Holt, R. M. and D.W. Powers, 1986, *Geotechnical activities in the Exhaust Shaft*, DOE-WIPP 86-008, U.S. Department of Energy, WIPP Project Office, Carlsbad, NM

Holt, R. M. and D.W. Powers. 1988. *Facies Variability and Post-Depositionsl Alteration Within the Rustler Formation in the Vicinity of the Waste Isolation Pilot Plant, Southeastern, New Mexico*. DOE-WIPP 88-004, U.S. DOE, WIPP Project Office, Carlsbad, NM.

Holt, R. M. and D.W. Powers. 1990. *Geologic mapping of the Air Intake Shaft at the Waste Isolation Pilot Plant, Southeastern New Mexico*. DOE-WIPP 90-051, US.S. Department of Energy, WIPP Project Office, Carlsbad, NM

Jones, T.L., V.A. Kelley, J.F. Pickens, D.T. Upton, R.L. Beauheim, and P.B. Davies. 1992. Integration of Interpretation Results of Tracer Tests Performed in the Culebra Dolomite at the Waste Isolation Pilot Plant Site, SAND92-1579.

Kelley, V.A. and G.J. Saulnier. 1990. *Core Analyses for Selected Samples from the Culebra Dolomite at the Waste Isolation Pilot Plant Site*. SAND90-7011.

Kloska, M.B., G.J. Saulnier, Jr., and R.L. Beauheim. 1995. *Culebra Transport Program Test Plan: Hydraulic Characterization of the Culebra Dolomite Member of the Rustler Formation at the H-19 Hydropad on the WIPP site.* (Results to be contained in WPO#s 38400 and 38401.)

Mercer, J.W. and B.R. Orr. 1979. *Interim data report on the geohydrology of the proposed Waste Isolation Pilot Plant Site in southeastern New Mexico*, U.S. Geological Survey Water Resources Investigations Report 79-89.

Stensrud, W.A., M.A. Bame, K.D. Lantz, J.B. Palmer, and G.J. Saulnier, 1990. *WIPP Hydrology Program, Waste Isolation Pilot Plant, Southeastern New Mexico, Hydrologic Data Report #8*, SAND89-7056.